Thermal transport in yttrium iron garnet at very high magnetic fields

D. R. Ratkovski [1,2] L. Balicas [1,*] A. Bangura,[1] F. L. A. Machado [1,2] and S. M. Rezende [2]

[1]*National High Magnetic Field Laboratory, Tallahassee, Florida 32310, USA*
[2]*Departamento de Física, Universidade Federal de Pernambuco, 50670-901, Recife, PE, Brazil*

The ferrimagnetic insulator yttrium iron garnet (YIG) is one of the most important materials in the active fields of insulator-based spintronics and spin caloritronics. Nevertheless, and despite the fact that this material has been studied for over six decades, the thermal properties of magnons in YIG have not been sufficiently characterized, mainly because at not very low temperatures they are overwhelmed by the contribution of phonons. Here, we report measurements of the thermal conductivity in YIG under magnetic fields up to 31.4 T to increase the magnon energy gap, to suppress the magnon contribution, and to isolate that of the phonons relative to their behavior at zero field. We observe that at a temperature of 20 K, even with a field as large as 31.4 T, the magnon contribution is not completely suppressed. The magnon thermal conductivity, measured by subtracting the value of the total thermal conductivity at 31.4 T from the value at zero field, has a peak at 16 K, with an amplitude that is over five times larger than the one obtained by measuring under a field of only 7 T, as previously reported.

I. INTRODUCTION

The ferrimagnetic insulator yttrium iron garnet ($Y_3Fe_5O_{12}$, or YIG) has been called the miracle material of microwave magnetics [1]. Since its discovery by Bertaut and Forrat in 1956 [2], more than any other material it has contributed to the understanding of spin waves and magnon dynamics due to its exceptionally low elastic and magnetic dampings [1,3–5]. The magnons are the quanta of magnetic oscillations in systems having a periodic array of ordered magnetic moments. More recently, yttrium iron garnet has become a key material for the understanding of phenomena associated with the emerging fields of insulator-based spintronics and spin caloritronics, such as the spin pumping [6–8] and the spin-Seebeck effects [8–15]. The recent upsurge in the interest in YIG has produced an intensification in the study of its basic properties, leading, for example, to the determination of its full magnon spectrum throughout the Brillouin zone via time-of-flight inelastic neutron scattering measurements [16]. One of the current challenges is to quantify the contribution of magnons to the thermal properties of YIG over a wide range of temperatures. This knowledge about their dynamics can be used to derive strict limitations on device performance and to determine the optimum operating conditions for magnonic nanostructures being proposed for data processing as the magnon transistor [17].

One aspect of the measurements of the thermal properties of YIG is that at temperatures above 5 K they are dominated by the behavior of the phonons, so that the contributions from magnons become difficult to determine. Early experimental attempts to characterize the magnon specific heat and thermal conductivity in YIG at temperatures (T) below 5 K employed the application of magnetic fields up to 4 T to open a gap in the magnon dispersion to freeze the magnon contributions and isolate those of the phonons relative to their behavior at zero field [18,19]. But even at low Ts it was recognized early on that the theory and the experimental data for the magnon thermal conductivity were discrepant [19]. Recently, Boona and Heremans [20] used a larger magnetic field (7 T) with the goal of freezing the magnon contributions claiming to have measured the absolute values of the magnon specific heat and thermal conductivity in YIG at temperatures up to 10 K. The experimental data of Ref. [20] were later contested by calculations that showed that they represented not absolute values, but only relative changes in the magnon contributions due to the application of the field [21].

In this paper, we report an investigation of the thermal conductivity of single-crystal yttrium iron garnet at low temperatures and very high magnetic fields. The main objective here is to determine the temperature and field dependencies of the magnon thermal conductivity. At a temperature $T = 10$ K, the measurements confirm the theoretical prediction [21] that a field of at least 30 T is necessary to decrease the magnon contribution to less than 10% of its zero-field value. At $T > 20$ K, even a field as high as 31.4 T is not enough to completely suppress the magnon contribution. The magnon thermal conductivity, measured by subtracting the value of the total thermal conductivity measured at the highest fields available from its values at zero field, has a peak at $T = 16$ K, with an amplitude that is over five times larger than the one obtained by measuring under a field of only 7 T [20].

II. EXPERIMENTAL RESULTS AND DISCUSSION

The measurements were performed in one sample of single-crystal [110] YIG with dimensions $3.0 \times 0.85 \times 0.48$ mm^3, obtained commercially from Airtron-Litton Ind. The thermal conductivity of the sample was measured using the same sample holder in two distinct experimental setups:
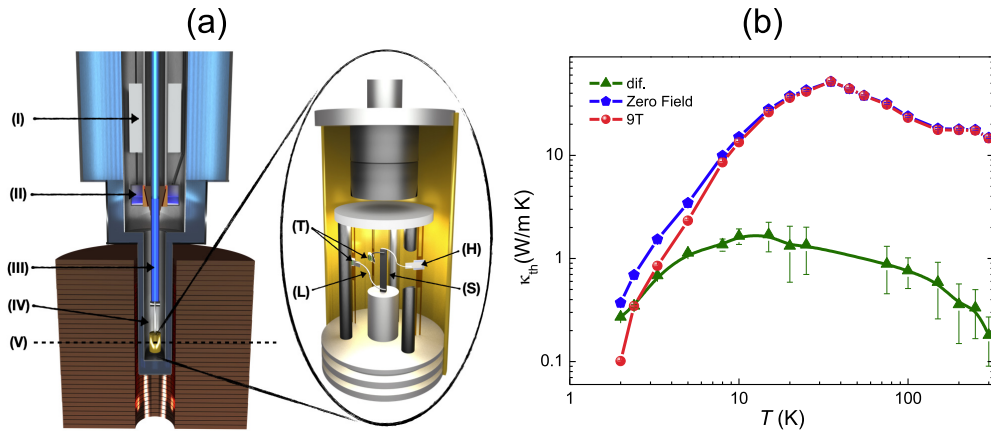
*balicas@magnet.fsu.edu

FIG. 1. (a) Schematic illustration of the apparatus and sample holder used for measuring the thermal conductivity κ_{th} of YIG at high magnetic fields, showing (I) sorb used both for injecting the exchange-gas and for producing high vacuum in the sample space; (II) 1 K pot used to condense ^{3}He inside the cold finger; (III) sample space; (IV) cold finger; and (V) center of the magnet with the sample holder. The zoom-in shows the sample holder with the YIG sample, the silver wires attached to the heater, and the Cernox thermometers, identified by the letters T for thermometers, L for thermal link, H for heater, and S for sample. (b) Temperature (T) dependence of κ_{th} measured in the PPMS under zero field (blue pentagons) and under a magnetic field of 9 T (red circles). The corresponding reduction in κ_{th} with the field is represented by the green triangles.

(a) in a Quantum Design Physical Property Measurement System (PPMS), with magnetic fields up to 9 T; and (b) in a Bitter resistive magnet providing fields up to 31.4 T at the National High Magnetic Field Laboratory in Tallahassee, FL. Figure 1(a) shows a schematic illustration of the ^{3}He insert in a Janis cryostat used for the measurements in the resistive magnet, as well as of the sample holder. The thermal conductivity was measured by injecting a heat power (P) in the hot end of the sample by means of a heater and measuring the corresponding temperature difference ΔT across the sample, using $\kappa_{th} = (l/tw)P/\Delta T$, where l, t, and w are, respectively, the length, thickness, and width of the sample. The contact of the heater to the sample was actually made with a silver wire attached to the sample with a high conductive silver epoxy (Epotek H20E), while the temperatures at the ends were measured using two Cernox thermometers, model CX-BC 1030, also in contact with the sample through silver wires. The magnetoresistances of the Cernox and of the heater were properly taken into consideration. All measurements reported here were performed under high vacuum in the sample space, because it was noticed that the exchange gas in the sample space drastically reduces the thermal gradient.

Figure 1(b) shows the temperature dependence of the thermal conductivity κ_{th} of the YIG sample in the range 2.4–300 K, measured in the PPMS, both in zero field and under a magnetic field $\mu_0 H = 9$ T. The measured conductivity is the sum of the contributions from phonons, κ_{ph}, and magnons, κ_m. The reduction in κ_{th} with the application of the field results from the decrease in κ_m due to the increase in the magnon energy and the consequent decrease in the magnon thermal population. The temperature dependence of κ_{th} in zero field and in an applied fields shown in Fig. 1(b) is qualitatively similar to the one reported in Ref. [20], but with a smaller magnitude. We attribute the smaller value of κ_{th} measured here to the fact that our experiments were done under high vaccum, while in Ref. [20] an exchange gas was used. Under exchange gas, we observe small differences between our data and those

displayed in Ref. [20], which we attribute to variations in sample quality.

Figure 2 shows the field dependence of κ_{th} at a constant temperature measured in the PPMS and in the resistive magnet. The measurements were performed under steady-state conditions at each temperature, by sweeping the field from -9 to $+9$ T in the PPMS, and from 0 to 31.4 T in the resistive magnet. Clearly, both data sets obtained in each setup agree quite well within the common field range used for the measurements.

The above measurements of the thermal conductivity in YIG can be understood in terms of the statistical theory for a noninteracting magnon gas [8,22]. First, we note that the thermal properties of magnons depend crucially on the wave-vector-dependent magnon frequency, velocity, and lifetime. The first two are given directly by the magnon dispersion relations, which have been recently recalculated for YIG and measured with modern inelastic neutron scattering techniques [18,23]. The data, which are in good agreement with the calculations, show an acoustic branch whose frequency increases from nearly zero (at zero field) at the Brillouin zone center to a value at the zone boundary (ZB) that varies from 6 to 9.5 THz depending on the wave-vector direction. These values correspond to energies of approximately 287 and 454 K, respectively. Since the lowest optical branch lies above the ZB value, the calculation of the thermal properties in the presence of an applied field $\mu_0 H$ at temperatures up to 100 K can be safely done considering only the acoustic branch [23,24]. Also, at low wave numbers the magnon dispersion relation can be approximated by the quadratic form [16]

$$\omega_k = \gamma \mu_0 H + \gamma D k^2, \tag{1}$$

where k is the wave number, D is the exchange parameter, $\gamma = g\mu_B/\hbar$ is the gyromagnetic ratio, g is the spectroscopic splitting factor, μ_B is the Bohr magneton, and the reduced Planck constant $\hbar$. Clearly, the application of a magnetic field creates in the magnon dispersion a frequency gap at $k = 0$
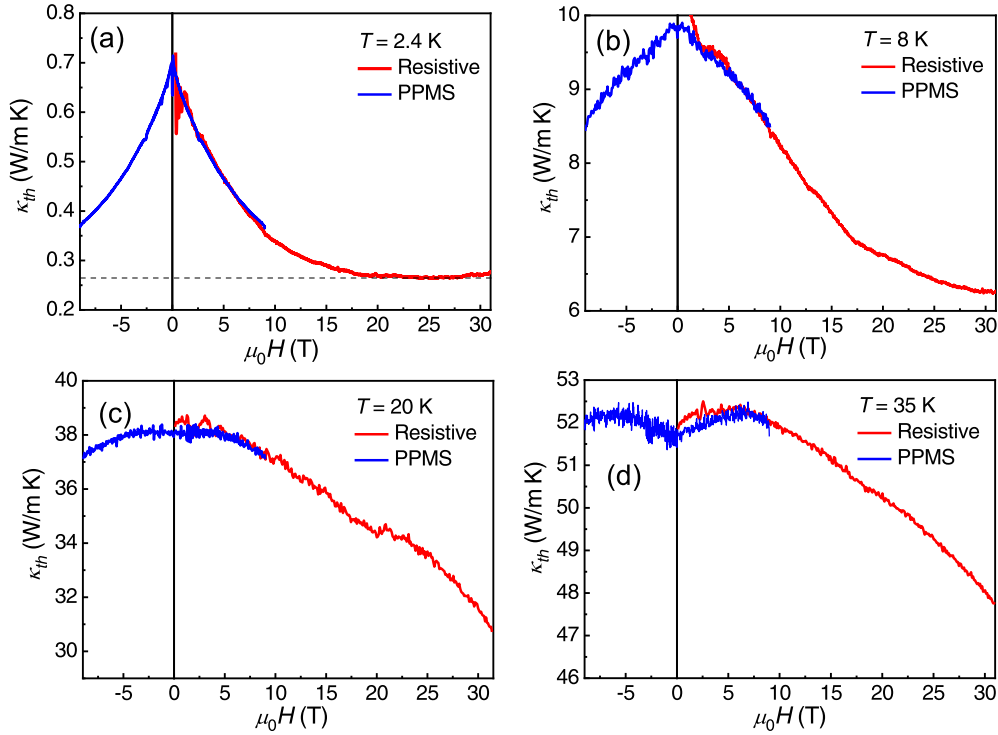
FIG. 2. Thermal conductivity κ_{th} of YIG as a function of the magnetic field measured at several temperatures both in a PPMS and in a resistive magnet.

of $\gamma\mu_0 H$, where $\gamma = 28$ GHz/T for YIG, corresponding to an energy of 1.34 K/T. The increased frequency reduces the number of thermal magnons at a temperature T, given by the Bose-Einstein distribution, $\bar{n}_q = 1/[\exp(\hbar\omega_q/k_B T) - 1]$. Thus, by applying a sufficiently large field at some T, the magnon contribution to the thermal properties can be largely reduced so that they become determined by phonons only. In this way, the changes in the thermal properties relative to the zero-field values would represent the magnetic contribution. While this is true, the values of the quenching fields used in Refs. [20,21] are underestimated. As shown in Ref. [22], with a field of 7 T the reduction in the magnon specific heat and thermal conductivity is less than 40% relative to the values at zero field.

For the calculation of the magnon thermal conductivity, one considers that the flow of magnons due to a temperature gradient ∇T carries a heat-current density $\vec{J}_Q = V^{-1}\sum_k \delta n_k \hbar\omega_k \vec{v}_k$, where $\delta n_k = n_k - \bar{n}_k$ is the magnon number in excess of equilibrium, and $\vec{v}_k$ is the k-magnon group velocity. Using the Boltzmann approach, one can write a first-order expression for the excess magnon number in the steady state and in the relaxation approximation, $\delta n_k = -\tau_k \vec{v}_k \cdot \nabla \bar{n}_k$, where τ_k is the k-magnon relaxation time. Assuming spherical magnon energy surfaces and considering for low T the quadratic dispersion in Eq. (1), one obtains a heat-current density in the form $\vec{J}_Q = -\kappa_m \nabla T$, where κ_m is the magnon thermal conductivity given by [8,25]

$$K_m = \frac{k_B (k_B T)^{5/2}}{3\pi^2 (\gamma D)^{1/2}\,\hbar^{5/2}} \int_{x_0}^{x_m} \frac{e^x x^2 (x-x_0)^{3/2}}{\eta_k (e^x - 1)^2}\, dx, \quad (2)$$

where $\eta_k = 1/\tau_k$ is the magnon relaxation rate and $x = \hbar\omega_k/k_B T$ is a dimensionless magnon energy. If one considers that the relaxation rate η_k is independent of the wave number and temperature, at zero field the lower limit of the integral is $x_0 = 0$, and at low temperatures the upper limit can be set to $x_m \to \infty$. In this case, the integral in Eq. (2) can be solved analytically to give $\Gamma(7/2)\varsigma(5/2)$, where the factors are, in order, the gamma and Riemann zeta functions. Thus, the temperature dependence of the magnon thermal conductivity is $\kappa_m \propto T^{5/2}$, first predicted by Yelon and Berger [25]. For nonzero field, the $T^{5/2}$ dependence still holds, but the amplitude decreases with field since $x_0 \propto H$ and x increases with field.

Actually, at temperatures $T > 5$ K, the magnons with larger wave numbers become important for the thermal conductivity so that the dependencies of the magnon relaxation rate on k, T, and H must be considered in the calculation [24]. A difficulty here is that the spin-wave damping has been measured experimentally only for very small wave numbers using microwave techniques [8], while the magnons that contribute most to the thermal conductivity are in the middle of the Brillouin zone. Thus, one has to resort to calculated relaxation rates, which are at best good estimates in the absence of data, and also adjust some parameters to the data. We have calculated the integral in Eq. (2) using the following expression for the magnon relaxation rate [24]

$$\eta_k = \eta_0 \left[1.0 + c_{H3} 7.5 \times 10^2 q\left(\frac{T}{300}\right) \right.$$
$$\left. + c_{H4} 10^3 (7.6q^2 - 4.9q^3)\left(\frac{T}{300}\right)^2 \right], \quad (3)$$
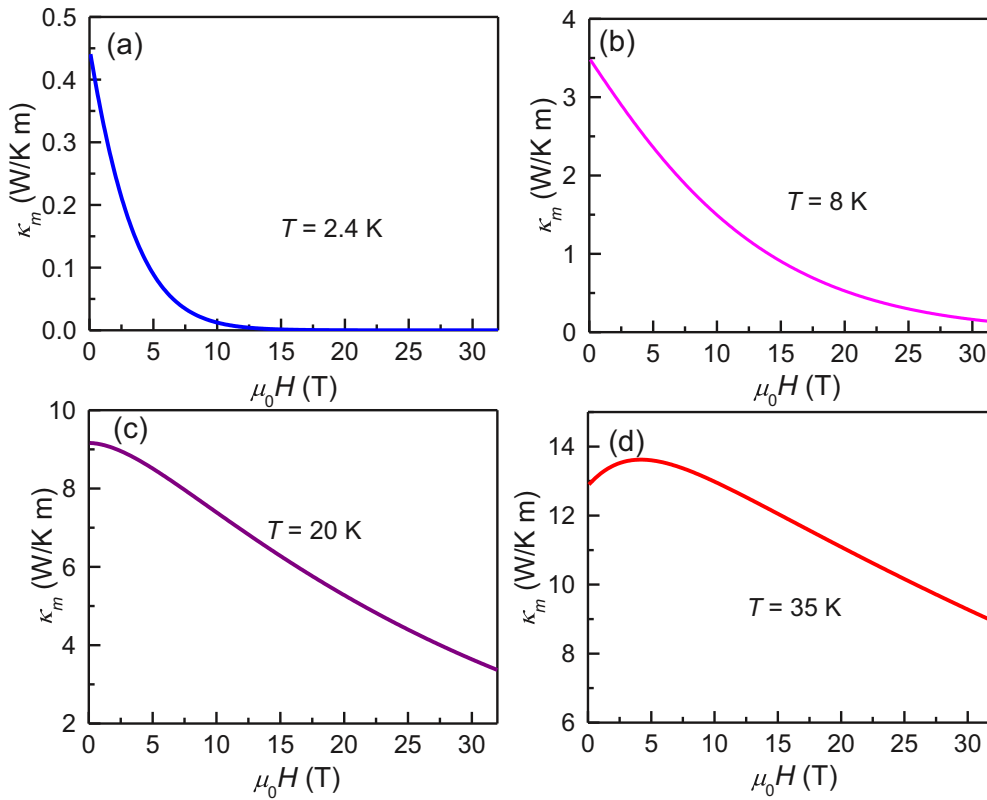
FIG. 3. Thermal conductivity in YIG as a function of the magnetic field at several temperatures and as calculated from Eqs. (1)–(3).

where η_0 is the relaxation rate at $k = 0$ and $T = 0$ due to impurities and other imperfections, while the second and third terms arise, respectively, from three- and four-magnon scattering processes. Equation (3) with $c_{H3} = c_{H4} = 1.0$ is the relaxation rate of Ref. [23] for $\mu_0 H = 0$. These factors were introduced here to account for the reduction of the damping with the application of a field. We have used $c_{H4} = 0.2 + 0.38\,e^{-0.3\mu_0 H} + 0.41\,e^{-0.01\mu_0 H}$ ($\mu_0 H$ in T), which was obtained by fitting two exponential functions to the four-magnon relaxation rate calculated numerically for the range of wave numbers $0.2 < k/k_{ZB} < 0.4$, and for $10 < T < 20$ K. Figure 3 shows the calculated field dependence of the magnon thermal conductivity for the same temperature values as in Fig. 2, using this expression for c_{H4}, $c_{H3} = 0.5$, $D = 5.4 \times 10^{-17}$ Tm^2, and $\gamma = 28$ GHz/T. The value of the magnon relaxation rate at $k = 0$ used in the calculation, $\eta_0 = 1.4 \times 10^8$ s^{-1}, was adjusted so as to obtain good agreement with the experimental data.

One can see from Fig. 3 that at $T = 2.4$ and 8 K, the calculated magnon thermal conductivity decays exponentially with increasing field, in quite good quantitative agreement with the variation of κ_{th} with H as shown Fig. 2. At these low temperatures the variation of the relaxation rate is small, so that the behavior of the conductivity is dominated by the decrease of the magnon thermal population with increasing field. Thus, for $T < 10$ K the magnon conductivity is suppressed by a field up to 35 T, so that its value in zero field can be reliably measured by subtracting the values of the total thermal conductivity at zero field and at $\mu_0 H = 35$ T. However, at larger temperatures the magnon contribution to the thermal

conductivity is not completely suppressed even under fields up to 35 T, as shown by the calculated behavior in Figs. 3(c) and 3(d), as well as by the data in Figs. 2(c) and 2(d). The main reason for this is that at higher temperatures the magnon conductivity is larger due to the $T^{5/2}$ factor, but the magnon relaxation decreases exponentially with increasing field, so that the overall behavior exhibits a peak before decreasing at higher fields.

The field dependence of the thermal conductivity measured at various temperatures, as seen in Fig. 2, was used to plot the variation with temperature of the difference between the conductivities at zero field and at selected field values. The results, shown in Fig. 4(a), reveal that only at $T < 3$ K is the magnon contribution to the thermal conductivity completely suppressed with a field of 7 T. For $T = 8$ K, complete suppression requires a field of at least 30 T, while for $T > 20$ K even this field value is not sufficient to achieve complete suppression. Notice also in Fig. 4(a) that the peak amplitude measured with a field of 30 T is over five times larger than the one measured with 7 T, indicating that the magnon thermal conductivity reported in Ref. [20] is underestimated, as pointed out in Ref. [21].

The inverted U-shaped behavior of the thermal conductivity difference in Fig. 4(a) is explained by the variation with temperature of the magnon contribution. At low Ts the conductivity increases with $T^{5/2}$ due to the increase in the magnon thermal population. At higher Ts the magnon relaxation increases so that the conductivity decreases. This behavior is reproduced qualitatively by the temperature dependence of the magnon thermal conductivity calculated through
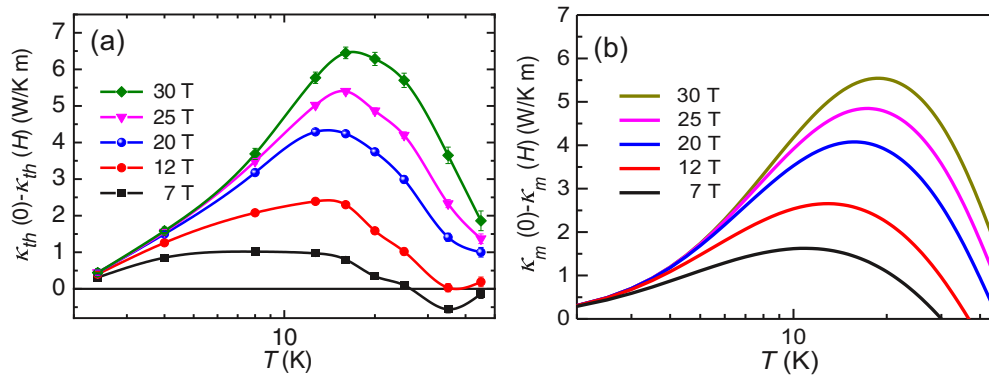
FIG. 4. (a) Difference between the thermal conductivities measured at zero field and under selected field values as a function of the temperature. (b) Temperature dependence of the calculated magnon thermal conductivity in YIG as a function of the temperature and for several field values.

Eqs. (1)–(3) under zero field and for several field values, as shown in Fig. 4(b).

III. SUMMARY

In summary, we have measured the thermal conductivity in single-crystalline yttrium iron garnet in the temperature range from 2.4 to 45 K under magnetic fields up to 31 T. Application of the field increases the magnon energies and reduces their contribution to the thermal properties. Our data show that at a temperature of 10 K, a field of at least 30 T is necessary to decrease the magnon contribution to less than 10% of its zero-field value. At $T > 20$ K even a field as high as 31 T is not enough to completely suppress the magnon contribution. The experimental data are quite well explained by a statistical theory for thermal transport in a noninteracting magnon gas. The magnon thermal conductivity, measured by subtracting the value of the total conductivity at the highest field available from the value at zero field, has a peak at $T = 16$ K, with an amplitude over five times larger than

the one obtained by measuring with a field of only 7 T as previously reported. In addition, the direct correlation of κ_{th} with phenomena induced by thermal currents makes the overall experimental results reported in the current work of great importance for researchers working with magnonics and in spintronics.

[1] A. V. Chumak, V. I. Vasyuchka, A. A. Serga, and B. Hillebrands, Magnon spintronics, Nat. Phys. **11**, 453 (2015).

[2] F. Bertaut and F. Forrat, Structure des ferrites ferrimagnetiques des terres rares, Compt. Rend. **242**, 382 (1956).

[3] J. R. Eshbach, Spin Wave Propagation and the Magnetoelastic Interaction in Yttrium Iron Garnet, Phys. Rev. Lett. **8**, 357 (1962).

[4] W. Strauss, Magnetoelastic waves in yttrium iron garnet, J. Appl. Phys. **36**, 118 (1965).

[5] S. M. Rezende and F. R. Morgenthaler, Magnetoelastic waves in time-varying magnetic fields. I. Theory, J. Appl. Phys. **40**, 524 (1969).

[6] Y. Kajiwara, K. Harii, S. Takahashi, J. Ohe, K. Uchida, M. Mizuguchi, H. Umezawa, K. Kawai, K. Ando, K. Takanashi, S. Maekawa, and E. Saitoh, Transmission of electrical signals by spin-wave interconversion in a magnetic insulator, Nature (London) **464**, 262 (2010).

[7] A. Hoffmann, Spin Hall effects in metals, IEEE Trans. Mag. **49**, 5172 (2013).

[8] S. M. Rezende, *Fundamentals of Magnonics* (Springer-Verlag, Berlin, 2020).

[9] K. Uchida, J. Xiao, H. Adachi, J. Ohe, S. Takahashi, J. Ieda, T. Ota, Y. Kajiwara, H. Umezawa, H. Kawai, G. E. W. Bauer, S. Maekawa, and E. Saitoh, Spin Seebeck insulator, Nat. Mater. **9**, 894 (2010).

[10] K. Uchida, H. Adachi, T. Ota, H. Nakayama, S. Maekawa, and E. Saitoh, Observation of longitudinal spin-Seebeck effect in magnetic insulators, Appl. Phys. Lett. **97**, 172505 (2010).

[11] G. E. W. Bauer, E. Saitoh, and B. J. van Wees, Spin caloritronics, Nat. Mater. **11**, 391 (2012).

[12] H. Adachi, K. Uchida, E. Saitoh, and S. Maekawa, Theory of the spin Seebeck effect, Rep. Prog. Phys. **76**, 036501 (2013).

[13] S. R. Boona, R. C. Myer, and J. P. Heremans, Spin caloritronics, Energy Environ. Sci. **7**, 885 (2014).

[14] T. Kikkawa, K.-i Uchida, S. Daimon, Z. Qiu, Y. Shiomi, and E. Saitoh, Critical suppression of spin Seebeck effect by magnetic fields, Phys. Rev. B **92**, 064413 (2015).

[15] S. M. Rezende, R. L. Rodríguez-Suárez, R. O. Cunha, A. R. Rodrigues, F. L. A. Machado, G. A. Fonseca Guerra, J. C. Lopez Ortiz, and A. Azevedo, Magnon spin-current theory for the longitudinal spin Seebeck effect, Phys. Rev. B **89**, 014416 (2019).

[16] A. J. Princep, R. A. Ewings, S. Ward, S. Tóth, C. Dubs, D. Prabhakaran, and A. T. Boothroyd, The full magnon spectrum of yttrium iron garnet, npj Quantum Mater. **2**, 63 (2017).

[17] A. V. Chumak, A. A. Serga, and B. Hillebrands, Magnon transistor for all-magnon data processing, Nat. Commun. **5**, 4700 (2014).

[18] R. L. Douglass, Heat transport by spin waves in yttrium iron garnet, Phys. Rev. **129**, 1132 (1963).

[19] D. Walton, J. E. Rives, and Q. Khalid, Thermal transport by coupled magnons and phonons in yttrium iron garnet at low temperatures, Phys. Rev. B **8**, 1210 (1973).

[20] S. R. Boona and J. P. Heremans, Magnon thermal mean free path in yttrium iron garnet, Phys. Rev. B **90**, 064421 (2014).

[21] S. M. Rezende and J. C. Lopez Ortiz, Thermal properties of magnons in yttrium iron garnet at elevated magnetic fields, Phys. Rev. B **91**, 104416 (2015).

[22] C. Kittel, *Quantum Theory of Solids*, 2nd revised printing (Wiley, New York, 1987).

[23] J. Barker and G. E. W. Bauer, Thermal Spin Dynamics of Yttrium Iron Garnet, Phys. Rev. Lett. **117**, 217201 (2016).

[24] S. M. Rezende, R. L. Rodríguez-Suárez, J. C. Lopez Ortiz, and A. Azevedo, Thermal properties of magnons and the spin Seebeck effect in yttrium iron garnet/normal metal hybrid structures, Phys. Rev. B **89**, 134406 (2014).

[25] W. B. Yelon and L. Berger, Magnon heat conduction and magnon scattering processes in Fe-Ni alloys, Phys. Rev. B **6**, 1974 (1972).